Electron–interface-phonon scattering in graded quantum wells of $Ga_{1-x}Al_xAs$

Wenhui Duan

Center of Theoretical Physics, Chinese Center of Advanced Science and Technology (World Laboratory),
P.O. Box 8730, Beijing 100080, China
*and Central Iron and Steel Research Institute, Beijing 100081, China**

Jia-Lin Zhu and Bing-Lin Gu

Center of Theoretical Physics, Chinese Center of Advanced Science and Technology (World Laboratory),
P.O. Box 8730, Beijing 100080, China
*and Department of Physics, Tsinghua University, Beijing 100084, China**

Using the method of series expansion, interface-phonon vibrational modes are calculated in the dielectric continuum model for the graded quantum well of $Ga_{1-x}Al_xAs$ with a $Ga_{0.6}Al_{0.4}As$ barrier. The intrasubband and intersubband scattering rates are obtained as functions of quantum-well width. The results reveal that the behavior of interface phonon modes is very different from that in a square quantum-well structure. It is found that the electron–interface-phonon scattering rates can be changed remarkably in a graded quantum-well structure compared with those in a square quantum-well structure, which is useful for some device applications.

I. INTRODUCTION

The scattering of electrons by polar optical phonons governs a number of important properties of semiconductor superlattice and quantum-well systems. In the systems, the presence of a heterointerface gives rise to the confinement of optical phonons in each layer and to localization in the vicinity of interfaces. Since unambiguous observation of the phonon confined in the GaAs slabs was made in 1984,[1] and interface phonons in GaAs-AlAs superlattices were discovered in 1985,[2] both macroscopic and microscopic approaches to confined phonons have been applied in the theoretical treatments, and the frequency and dispersion of the interface modes have been analyzed in terms of the dielectric continuum model.[3–13] Much of the research work concerning phonon modes has focused on their role in intrasubband and intersubband electron-phonon scattering. The studies have shown that the continuum model gives a reasonably good representation of these modes. It has been well recognized that the phonon modes in superlattice and quantum-well systems are evidently different from those in the bulk, and their interaction with electrons is modified because of reduced dimensionality. Recently, it has been found that metal-semiconductor heterointerface introduced in quantum-well systems can also modify interface-phonon modes.[14–16]

Among the superlattice and quantum-well systems, the square-quantum-well (SQW) structures have frequently been studied by a number of techniques. In 1983, Capasso et al.[17] observed a transient electrical polarization phenomenon in sawtooth superlattices of $Ga_{1-x}Al_xAs$, which drew attention to some interesting device application of graded-gap structures. Since then, the electronic structure and related phenomenon of the graded-gap systems have been studied.[18–25] In order to achieve high de-

vice performances, such as high on-off ratio and a low operation voltage, Polland et al.,[18] Nishi and Hiroshima,[21] and Zhu, Tang, and Gu[22] have proposed a graded quantum-well (GQW) structure, where the conduction- and valence- band edges vary linearly along the growth direction in the well layer. The electron and exciton states in the GQW structure with or without electric field were investigated in detail. It is shown that the lack of planes of reflection symmetry in such a structure, compared with a conventional SQW structure, can open the door to a number of exciting new effects. However, to our knowledge, no quantitative descriptions are available for optical-phonon modes in the GQW structure. It would be expected that the difference between GQW and SQW structures will result in a significant change of subband wave functions and optical phonons and related electron–optical-phonon interactions, which are important for electron relaxation and mobility. Therefore, it should be worthwhile investigating the optical-phonon modes and their effect on electron relaxation in a GQW structure.

In the present paper, we study the interface phonon and related electron-phonon scattering in the dielectric continuum model for GQW of $Ga_{1-x}Al_xAs$. The method of series expansion[26] is used to calculate dispersion relations of vibrational modes and electron subband wave functions. The intrasubband and intersubband scattering rates in the GQW structure are obtained, and the effect of well shape on the scattering is discussed.

II. INTERFACE-PHONON MODES AND ELECTRON SUBBANDS

In the theoretical calculation, an isolated GQW of $Ga_{1-x}Al_xAs$ between infinite $Ga_{1-y}Al_yAs$ barrier layers is taken and its Al content x varies continuously from 0

to x_0 along the growth direction (z axis), i.e.,

$$x = \frac{z}{a}x_0 \quad 0 < z < a \ , \tag{1}$$

where a is the width of well region. The potential height $V(x)$ (in units of eV) and the optical dielectric constant $\epsilon_\infty(x)$ have, respectively, the forms[27]

$$V(x) = (1.115x + 0.37x^2)Q$$

$$= \left[1.115x_0\frac{z}{a} + 0.37x_0^2\left[\frac{z}{a}\right]^2\right]Q \tag{2}$$

and

$$\epsilon_\infty(x) = 10.89 - 2.73x = 10.89 - 2.73x_0\frac{z}{a} \ , \tag{3}$$

where Q is the conduction-band offset parameter and, in general, is taken to be 0.6. The corresponding LO and TO phonon frequencies $\omega_L(x)$ and $\omega_T(x)$ (in units of cm^{-1}) have taken the forms[27]

$$\omega_L(x) = 292.37 - 52.83x_0\frac{z}{a} + 14.44x_0^2\left[\frac{z}{a}\right]^2$$

for GaAs-like modes   (4a)

$$\omega_L(x) = 359.96 + 70.81x_0\frac{z}{a} - 26.78x_0^2\left[\frac{z}{a}\right]^2$$

for AlAs-like modes   (4b)

and

$$\omega_T(x) = 268.50 - 5.16x_0\frac{z}{a} - 9.36x_0^2\left[\frac{z}{a}\right]^2$$

for GaAs-like modes   (5a)

$$\omega_T(x) = 359.96 + 4.44x_0\frac{z}{a} - 2.42x_0^2\left[\frac{z}{a}\right]^2$$

for AlAs-like modes ,   (5b)

respectively. The effective mass $m(x)$ (in units of free-electron mass) of an electron is as follows:

$$m(x) = 0.067 + 0.083x = 0.067 + 0.083x_0\frac{z}{a} \ . \tag{6}$$

Within the framework of the continuum model,[5,8] the coupled integral equation of motion for polarization eigenmodes can be obtained. Introducing the electric-field component $E_k(\mathbf{k},z)$ and the electric displacement component $D_z(\mathbf{k},z)$, where $\mathbf{k}$ is the in-plane component of the phonon wave vector, and differentiating the coupled integral equation with respect to z, we have

$$\frac{dE_k}{dz} = ik\frac{D_z}{\epsilon} \ ,$$

$$\frac{dD_z}{dz} = -ik\epsilon E_k \ , \tag{7}$$

with

$$\epsilon(\omega) = \epsilon_\infty\frac{\omega_L^2 - \omega^2}{\omega_T^2 - \omega^2} \ . \tag{8}$$

Noting that dielectric function ϵ is the function of z in the well region, the decoupled differential equations can be obtained from Eqs. (7) and (8) as follows:

$$\frac{d^2E_k}{dz^2} + \frac{1}{\epsilon}\frac{d\epsilon}{dz}\frac{dE_k}{dz} - k^2E_k = 0 \ , \tag{9a}$$

$$\frac{d^2D_z}{dz^2} - \frac{1}{\epsilon}\frac{d\epsilon}{dz}\frac{dD_z}{dz} - k^2D_z = 0 \ . \tag{9b}$$

Considering that Al content in well region is small, we omit the z^2 items in Eqs. (4) and (5) for the convenience of calculation. Substituting Eq. (8) into Eq. (9a), we have

$$\left[\sum_{l=0}^{5}p_lz^l\right]\frac{d^2E_k}{dz^2} + \left[\sum_{l=0}^{4}q_lz^l\right]\frac{dE_k}{dz} - k^2\left[\sum_{l=0}^{5}p_lz^l\right]E_k = 0 \ , \tag{10}$$

where p_l and q_l are constants determined by ω and x_0. For the sake of better numerical computations, we rewrite Eq. (10) to

$$\left[\sum_{l=0}^{5}r_l(z-z_0)^l\right]\frac{d^2E_k}{dz^2} + \left[\sum_{l=0}^{4}t_l(z-z_0)^l\right]\frac{dE_k}{dz}$$

$$-k^2\left[\sum_{l=0}^{5}r_l(z-z_0)^l\right]E_k = 0 \ , \tag{11}$$

where z_0 is a constant, r_l and t_l are constants dependent on z_0. Expanding E_k as a uniformly convergent Taylor series, and substituting it into Eq. (11), we get the solution as follows:[26]

$$E_k = C_1\sum_{n=0}^{\infty}u_n(z-z_0)^n + C_2\sum_{n=0}^{\infty}v_n(z-z_0)^n \tag{12}$$

with

$$\begin{cases}u_0 = 1, & u_1 = 0 \\ v_0 = 0, & v_1 = 1 \ ,\end{cases} \tag{13}$$

where C_1 and C_2 are constants, u_n and v_n are the coefficients of the series solution which can be determined by the recurrence relation. E_k and D_z in the barrier region can also be deduced from Eqs. (9a) and (9b) with ϵ independent of z. Therefore, the E_k in the GQW structure takes the form

$$E_k = \begin{cases}Ae^{kz}, & z < 0 \\ C_1\displaystyle\sum_{n=0}^{\infty}u_n(z-z_0)^n + C_2\displaystyle\sum_{n=0}^{\infty}v_n(z-z_0)^n \ , \\ \qquad\qquad\qquad\qquad 0 \le z \le a \\ Be^{-kz}, & z > a\end{cases} \tag{14}$$

and the D_z can be obtained from E_k by use of Eq. (7). By using the connection condition of E_k and D_z, the equation of dispersion relation for interface phonon is obtained as follows:

$$\left[M_{11}+M_{12}\frac{k\epsilon_0}{\epsilon(0)}\right]\frac{k\epsilon_0}{\epsilon(x_0)}+M_{21}+M_{22}\frac{k\epsilon_0}{\epsilon(0)}=0 , \qquad (15)$$

where ϵ_0 is the dielectric function in the barrier region, $\epsilon(0)$ and $\epsilon(x_0)$ are the dielectric functions at $z=0$ and $z=a$, and M_{ij} is an element of the 2×2 matrix M. It is as follows:

$$M=\begin{bmatrix} M_{11} & M_{12} \\ M_{21} & M_{22} \end{bmatrix}$$

$$= \begin{vmatrix} \displaystyle\sum_{n=0}^{\infty} u_n(a-z_0)^n & \displaystyle\sum_{n=0}^{\infty} v_n(a-z_0)^n \\ \displaystyle\sum_{n=0}^{\infty} nu_n(a-z_0)^{n-1} & \displaystyle\sum_{n=0}^{\infty} nv_n(a-z_0)^{n-1} \end{vmatrix}$$

$$\times \begin{vmatrix} \displaystyle\sum_{n=0}^{\infty} u_n(-z_0)^n & \displaystyle\sum_{n=0}^{\infty} v_n(-z_0)^n \\ \displaystyle\sum_{n=0}^{\infty} nu_n(-z_0)^{n-1} & \displaystyle\sum_{n=0}^{\infty} nv_n(-z_0)^{n-1} \end{vmatrix} . \qquad (16)$$

With the use of Eq. (15) and the normalization condition,[5,8] the eigenvalue ω_ν, the constants A, B, C_1 and C_2 (hence E_k and D_z) are determined.

Effective-mass theory is used to calculate the subband wave functions of electron states. The envelope subband wave function satisfies

$$\frac{\hbar^2}{2m}\frac{d^2\Psi}{dz^2}+V\Psi=E_e\Psi . \qquad (17)$$

It must be noted that V and m are the functions of z. Using the method of series expansion in a calculation procedure similar to that of interface modes calculation, Eq. (17) can be solved and electron subband wave functions can be obtained, which has been discussed in detail in the previous papers.[22,23] It is interesting to point out that the similarity of calculation method for electron wave function and interface modes will make it convenient to calculate the scattering rate.

III. THE ELECTRON-INTERFACE PHONON SCATTERING

The electron-phonon interaction Hamiltonian derived from Fröhlich interaction has been given by several authors.[4–6,8] A very complete analysis of effective electron-phonon interaction has been done on the basis of the important sum rule,[8] which is convenient and useful for understanding the relative importance of interface modes and confined modes. The same kind of Hamiltonian is used in this paper. For the sake of numerical calculations,[12] however, it is given by

$$H_{ep}=\sum_\nu\sum_k \left[\frac{\hbar e^2}{2A\omega_\nu(k)}\right]^{1/2}\frac{i}{k}E_k^\nu(k,z)$$

$$\times e^{ik\cdot\rho}[a_\nu(k)+a_\nu^\dagger(-k)] \qquad (18)$$

where ν refers to the possible solutions of Eq. (15), a_ν and $a_\nu^\dagger$ are, respectively, the annihilation and creation operator of the νth optical-phonon mode, and A is unit area of the quantum-well system in the xy plane. Considering one phonon process only with the standard manner, the scattering rate is obtained as follows:

$$W(k_e)=\frac{2\pi}{\hbar}\int dN_f\delta[E_{Tf}-E_{Ti}\pm\hbar\omega(k)]|\langle k_e'|H_{ep}|k_e\rangle|^2$$

$$=\frac{e^2\epsilon_0}{4\pi}\sum_\nu\int d^2k\frac{1}{\omega_\nu(k)k^2}|F_\nu(k)|^2$$

$$\times\delta[E_{Tf}-E_{Ti}\pm\hbar\omega_\nu(k)]$$

$$\times\left[N_{ph}+\frac{1}{2}\mp\frac{1}{2}\right]\delta_{k_e,k_e'\mp k} \qquad (19)$$

with

$$F_\nu(k)=\int_{-\infty}^{\infty} dz\Psi_f^*(z)E_k^\nu(k,z)\Psi_i(z) , \qquad (20)$$

where the upper (lower) sign is for phonon emission (absorption), and $i(f)$ sign denotes the initial (final) state. E_T is the electron energy and taken to be $(E+\hbar^2k_e^2/2m^*)$, where m^* is the effective mass of an electron in the xy plane and E is the electron subband energy. $\Psi(z)$ is the normalized wave function. N_{ph} stands for the number of phonons.

For the intrasubband scattering within the first subband, we consider the scattering rate W_{11} for phonon emission. Assuming that the electron energy is just enough to emit one interface phonon, we can obtain

$$W_{11}(k_{11})=\sum_\nu\frac{e^2\epsilon_0}{2\omega_\nu(k_{11})k_{11}}\left[\frac{\hbar^2}{m^*}k_{11}-\hbar\frac{d\omega_\nu}{dk}\bigg|_{k=k_{11}}\right]^{-1}$$

$$\times|F_\nu(k_{11})|^2(N_{ph}+1) , \qquad (21)$$

where k_{11} satisfies

$$(\hbar^2/2m^*)k_{11}^2-\hbar\omega_\nu(k_{11})=0 . \qquad (22)$$

For the intersubband transition between the first and second subbands, we consider the scattering rate W_{21} still for phonon emission. Assuming that the electron is initially at the bottom of the second subband, we have

$$W_{21}(k_{21})=\sum_\nu\frac{e^2\epsilon_0}{2\omega_\nu(k_{21})k_{21}}\left[\frac{\hbar^2}{m^*}k_{21}+\hbar\frac{d\omega_\nu}{dk}\bigg|_{k=k_{21}}\right]^{-1}$$

$$\times|F_\nu(k_{21})|^2(N_{ph}+1) , \qquad (23)$$

where k_{21} satisfies

$$(\hbar^2/2m^*)k_{21}^2+\hbar\omega_\nu(k_{21})-(E_2-E_1)=0 \qquad (24)$$

and (E_2-E_1) is the energy difference between the first and second subbands.

IV. RESULTS AND DISCUSSION

It has been found that the phonons are primarily AlAs-like as the Al content x is larger and they are primarily GaAs-like as x is smaller.[28,29] In the present work, the GaAs-like interface phonons and the corresponding electron-phonon scattering rates are studied for

$Ga_{0.6}Al_{0.4}As/Ga_{1-x}Al_xAs/Ga_{0.6}Al_{0.4}As$ GQW structures with $x_0 = 0.1$, $x_0 = 0.15$, and $x_0 = 0.2$. For the sake of comparison, a similar calculation is also performed for $Ga_{0.6}Al_{0.4}As/GaAs/Ga_{0.6}Al_{0.4}As$ SQW structure.

A sketch of the confining potential and related electron wave functions are shown in Fig. 1. It is clearly shown that the wave functions of the first and second subbands in the GQW structure are localized on the left side of the well region and different from those in the SQW structure.

In Fig. 2(a), the dispersion curves of interface modes in the GQW and SQW structures mentioned above have been given. It can be seen that the dispersion relations are dependent on the gradient of the GQW. There are two interface modes with frequency magnitude between $\omega_L(0.4)$ and $\omega_L(x_0)$ and two with frequency magnitude between $\omega_T(0.4)$ and $\omega_T(x_0)$. The limiting frequencies approach to the LO and TO frequencies of the $Ga_{0.6}Al_{0.4}As$ and $Ga_{1-x_0}Al_{x_0}As$ materials as ka approaches to zero. It is interesting to note that the interface mode with frequency near $\omega_L(x_0)$ is almost dispersionless as x_0 takes a relative great value. In fact, the dispersion in GQW structure reduces as x_0 (the gradient of GQW) increases. When $x_0 \geq y(0.4)$, there are no interface modes which can propagate in the whole system and take the maximum at the interface.

In Fig. 2(b), the electric-field components E_k of interface modes with $ka = 0.6$ are given for the GQW structures with $x_0 = 0.1$ and $x_0 = 0.2$. It is shown that mode 4 whose frequency is the highest among four modes is sensitive to x_0 (i.e., the gradient of the GQW). In fact, the mode in the SQW structure is antisymmetric, while the mode in the GQW structure becomes more symmetric in the well region with increasing x_0. The change of the other three modes is relatively small. It can be found that modes 3 and 4 are much more important than modes 1 and 2 for electron-phonon scattering induced by Fröhlich interaction.
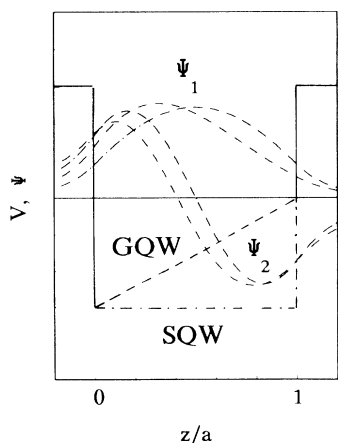

FIG. 2. (a) Dispersion relations of the interface modes in $Ga_{0.6}Al_{0.4}As/Ga_{1-x}Al_xAs/Ga_{0.6}Al_{0.4}As$ GQW structures with $x_0 = 0.1$ (solid curves) and $x_0 = 0.2$ (dashed curves). The dashed-dotted curves represent ones in $Ga_{0.6}Al_{0.4}As/GaAs/Ga_{0.6}Al_{0.4}As$ SQW structure. (b) Electric-field components E_k of interface modes with $ka = 0.6$ as a function of z in the same GQW structures as those in Fig. 1. The numbers on curves present the modes in order of increasing magnitude of frequency. It is the same in Figs. 3 and 4.

FIG. 1. Sketch of the confining potential V, the first-subband electron wave function Ψ_1 and the second-subband wave function Ψ_2 for $Ga_{0.6}Al_{0.4}As/Ga_{1-x}Al_xAs/Ga_{0.6}Al_{0.4}As$ GQW structure with $x_0 = 0.2$ (dashed curves) and the SQW structure (dashed-dotted curves). The well width a is taken to be 90 Å.
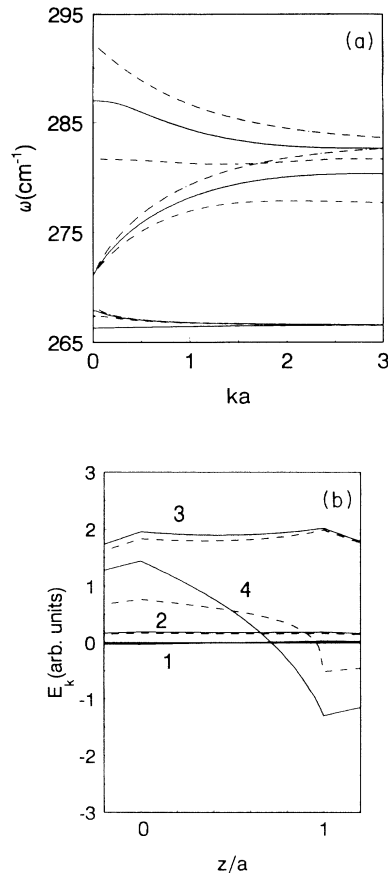
The intrasubband and intersubband scattering rates divided by $(N_{ph} + 1)$ in the GQW structure with $x_0 = 0.1$, $x_0 = 0.15$, and $x_0 = 0.2$ are calculated for each interface mode, as shown in Figs. 3 and 4, respectively. The contribution of the modes 1 and 2 to scattering can be ignored and are not shown in the figures. It is found that both modes 3 and 4 in the GQW structure contribute to the intrasubband and intersubband scatterings. In the SQW structure, due to parity-based selection rules, the intrasubband scattering within the first electron subband is restricted to symmetric modes and the intersubband scattering between the first and the second electron subband is restricted to antisymmetric modes. In the GQW structure, however, the reflection symmetry of structure (hence selection rules) is destroyed and all modes can contribute to the both kinds of scatterings. The E_k of mode 3 becomes more asymmetric and localized on the right-hand side of the well region with increasing x_0 and ka. Therefore, the intrasubband scattering rate W of
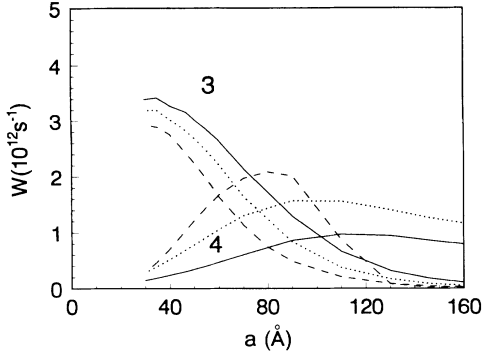
FIG. 3. Intrasubband scattering rates of interface modes 3 and 4 as a function of well width a in the GQW structure with $x_0=0.1$ (solid curves), 0.15 (dotted curves), and 0.2 (dashed curves).

mode 3 decreases with increasing well width a or Al content x_0, as shown in Fig. 3. However, the W of mode 4 increases with increasing a until its maximum and, then, decreases with increasing a. The W of mode 4 increases with increasing x_0 as the well width a is less than about 100 Å, and the W with larger x_0 can be less than that with smaller x_0 as the well width a becomes larger. It is easy to understand if the changes of the electron wave function and the interface-phonon mode 4 with x_0 and a are noted. With increasing x_0, the wave functions become more localized on the left side with smaller Al content as shown in Fig. 1 while the E_k of interface-phonon mode 4 becomes more symmetric and more flat and small on the left-hand side of the well region as shown in Fig. 2(b). The change of symmetry can make the W of mode 4 increase, and the increase of well width a and the decrease of E_k make the W decrease. This is the reason why there is a maximum for the W of mode 4.

In Fig. 4, it is shown that the intersubband scattering rate W of mode 4 decreases with increasing x_0, and that the variation of W in GQW structure of $x_0=0.1$ and $x_0=0.15$ with well width a is somewhat similar to that in SQW structure ($x_0=0$). It seems to be surprising that

the W of mode 4 in GQW structure with $x_0=0.2$ is very small and almost equal to zero for $a>70$ Å. It, in fact, can be explained by the fact that the value of E_k of mode 4 in GQW structure with $x_0=0.2$ is small and very close to a constant on the left-hand side of the well region where the electron wave functions are localized as mentioned above and it makes the overlap integral $F_v(k)$ of Eq. (20) closer to zero because of the orthogonality of the wave functions. The values of mode 3 are small compared with those of mode 4 of $x_0=0.1$ and 0.15 in all of the region of the figure. It is interesting to note that the W increases with decreasing x_0 even though it is equal to zero for $x_0=0$, i.e., SQW. This shows that $F_v(k_{12})$ of Eq. (23) is dependent on not only the symmetry of E_k but also its values in the region where the wave functions of the first and second subbands are mainly localized. In addition, it is also interesting to point out that there is only one subband energy level and no intersubband scattering for such a barrier layer $Ga_{0.6}Al_{0.4}As$ with the well width a less than about 50 Å.

In Fig. 5, the intrasubband scattering rates divided by $(N_{ph}+1)$ are given for interface modes in the SQW and GQW structures with $x_0=0.1, 0.15$, and 0.2. It is readily seen that as the well width a is less than 100 Å, the scattering rates in GQW structures are almost the same as those in the SQW structure. It is interesting to find that as the well width is larger, the scattering rates in the GQW structure with $x_0=0.2$ are rather small compared with those in the GQW structure with $x_0=0.1$ and 0.15 and those in the SQW structure. It can be explained from Fig. 3. In Fig. 6, the intersubband scattering rates divided by $(N_{ph}+1)$ are given for interface modes in the same GQW and SQW structures as those in Fig. 5. We can find that the intersubband scattering rates in the GQW structure with $x_0=0.2$ are quite different from those in the GQW structure with $x_0=0.1$ and 0.15 and those in the SQW structure. A much longer intersubband relaxation time can be expected in the GQW structure with $x_0=0.2$. It can be explained from Fig. 4.

For the AlAs-like interface phonons and related scattering rates, the same kinds of calculations can be
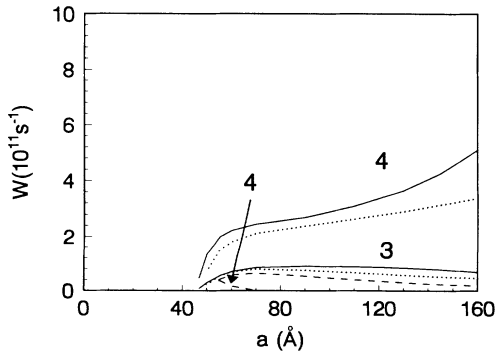

FIG. 4. Intersubband scattering rate of interface modes as a function of well width a in the GQW structure with $x_0=0.1$ (solid curves), 0.15 (dotted curves), and 0.2 (dashed curves).
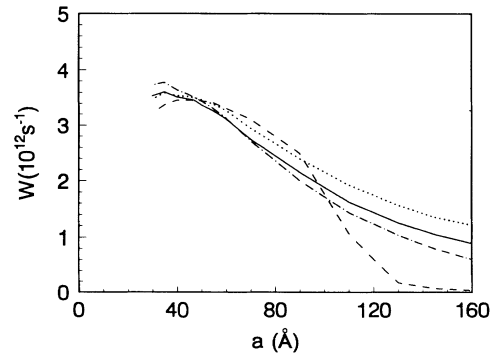

FIG. 5. Intrasubband scattering rates as a function of well width a in the GQW structures with $x_0=0$ (dashed-dotted curves), 0.1 (solid curves), 0.15 (dotted curves), and 0.2 (dashed curves).
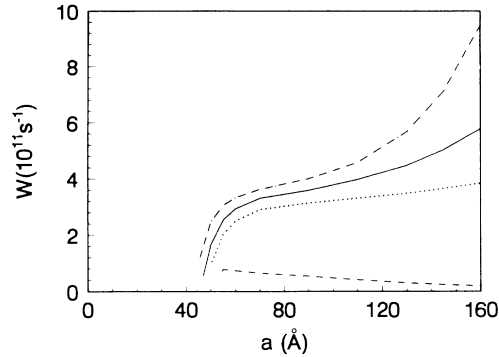
FIG. 6. Intersubband scattering rates as a function of well width a in the GQW structures with $x_0=0$ (dashed-dotted curves), 0.1 (solid curves), 0.15 (dotted curves), and 0.2 (dashed curves).

done by using Eqs. (4b) and (5b) instead of Eqs. (4a) and (5a). It is important to point out that the effect of a graded quantum well on the AlAs-like interface modes is different from that on the GaAs-like interface modes since the LO frequency $\omega_L(x)$ and TO frequency $\omega_T(x)$ of GaAs-like phonons decrease and those of AlAs-like phonons increase with increasing x as shown in Eqs. (4)

and (5). However, the analysis is similar to what we have mentioned above.

In conclusion, we have investigated quantitatively the behavior of interface phonon and its influence on electron scattering in GQW structures. It has been shown that the dispersion relations of interface modes in GQW structures are dependent on the gradient of the GQW and quite different from those in SQW structures. For different interface modes in GQW structures, the influence of well shape on dispersion relation and electric-field component is different. Some modes are sensitive to the gradient of the GQW, and the others are not. Thus the electron-interface phonon scatterings in the GQW structures are dependent on the properties (in particular, the gradient of the GQW) of materials which form the quantum-well system, and can be quite different from those in the SQW structure. The influence of interface phonon on electron scattering and relaxation can be reduced remarkably in a proper chosen GQW structure. Since the interface-phonon scattering is the important scattering mechanism in quantum-well systems,[8,10-13] the investigation of interface-phonon modes and related electron-phonon scattering in GQW structures is useful for some device applications. In addition, it is interesting to point out that the calculating method used here can be used for the study of interface-phonon behavior in other kinds of quantum-well structures.

*Mailing address.

[1] B. Jusserand, D. Paquet, and A. Regreny, Phys. Rev. B 30, 6245 (1984).

[2] A. K. Sood, J. Menéndez, M. Cardona, and K. Ploog, Phys. Rev. Lett., 54, 2115 (1985).

[3] R. Fuchs and K. L. Kliewer, Phys. Rev. 140, A2076 (1965).

[4] J. J. Licari and R. Evrard, Phys. Rev. B 15, 2254 (1977).

[5] L. Wendler, Phys. Status Solidi B 129, 513 (1985).

[6] K. Huang and B. Zhu, Phys. Rev. B 38, 2183 (1988); 38, 13 377 (1988).

[7] B. K. Ridley, Phys. Rev. B 39, 5282 (1989).

[8] N. Mori and T. Ando, Phys. Rev. B 40, 6175 (1989).

[9] R. Chen, D. L. Lin, and T. F. George, Phys. Rev. B 41, 1435 (1990).

[10] S. Rudin and T. L. Reinecke, Phys. Rev. B 41, 7713 (1990).

[11] K. J. Nash, Phys. Rev. B 46, 7723 (1992).

[12] W. Duan, J.-L. Zhu, and B.-L. Gu, J. Phys. Condens. Matter 5, 2859 (1993).

[13] J. L. Educato, J. P. Leburton, P. Boucaud, P. Vagos, and F. H. Julein, Phys. Rev. B 47, 12 949 (1993).

[14] M. A. Stroscio, K. W. Kim, G. J. Iafrate, M. Dutta, and H. L. Grubin, Philos. Mag. Lett. 65, 173 (1992).

[15] A. R. Bhatt, K. W. Kim, M. A. Stroscio, G. J. Iafrate, M. Dutta, H. L. Grubin, R. Haque, and X. T. Zhu, J. Appl. Phys. 73, 2338 (1993).

[16] N. C. Constantinou, Phys. Rev. B 48, 11 931 (1993).

[17] F. Capasso, S. Luryi, W. T. Tsang, C. G. Bethea, and B. F. Levine, Phys. Rev. Lett. 51, 2318 (1983).

[18] H.-J. Polland, L. Schultheis, J. Kuhl, E. O. Gobel, and C. W. Tu, Ultrafast Phenomena, edited by G. R. Fleming and A. E. Siegmann (Springer, Berlin, 1986), p. 234.

[19] M. Jaros, K. B. Wong, and M. A. Gell, J. Vac. Sci. Technol. B 3, 1051 (1985).

[20] V. Milanovic, Z. Ikonic, and D. Tjapkin, Phys. Rev. B 36, 8155 (1987).

[21] K. Nishi and T. Hiroshima, Appl. Phys. Lett. 51, 320 (1987).

[22] J.-L. Zhu, D. H. Tang, and B.-L. Gu, Phys. Rev. B 39, 3896 (1989).

[23] J.-L. Zhu, J. J. Xiong, and B.-L. Gu, J. Phys. Condens. Matter 1, 7595 (1989).

[24] F. M. Peeters, A. Kastalsky, W. Xu, and J. T. Devreese (unpublished).

[25] M. R. Geller and W. Kohn, Phys. Rev. Lett. 70, 3103 (1993).

[26] J.-L. Zhu, B.-L. Gu, and Y. M. Lou, Phys. Lett. 142, 159 (1989).

[27] S. Adachi, J. Appl. Phys. 58, R1 (1986).

[28] J. A. Kash, S. S. Jha, and J. C. Tsang, Phys. Rev. Lett. 58, 1869 (1987).

[29] P. J. Turley and S. W. Teitsworth, Phys. Rev. B 44, 3199 (1991).